

See discussions, stats, and author profiles for this publication at: <https://www.researchgate.net/publication/231234142>

Flammability Properties of Polymer–Layered–Silicate Nanocomposites. Polypropylene and Polystyrene Nanocomposites†

ARTICLE in CHEMISTRY OF MATERIALS · JULY 2000

Impact Factor: 8.35 · DOI: 10.1021/cm0001760

CITATIONS

1,060

READS

796

4 AUTHORS, INCLUDING:



Jeffrey W Gilman

National Institute of Standards and Technolo...

150 PUBLICATIONS 7,182 CITATIONS

SEE PROFILE



Catheryn Jackson

Dow Chemical Company

30 PUBLICATIONS 2,862 CITATIONS

SEE PROFILE



Alexander B. Morgan

University of Dayton

76 PUBLICATIONS 4,575 CITATIONS

SEE PROFILE

Flammability Properties of Polymer–Layered-Silicate Nanocomposites. Polypropylene and Polystyrene Nanocomposites[†]

Jeffrey W. Gilman,^{*,‡,||} Catheryn L. Jackson,^{§,||} Alexander B. Morgan,^{‡,||} and Richard Harris, Jr.^{‡,||}

Fire Science Division, Building and Fire Research Laboratory, and Polymers Division, Materials Science and Engineering Laboratory, National Institute of Standards and Technology, Gaithersburg, Maryland 20899

Evangelos Manias

Materials Science and Engineering Department, Pennsylvania State University, University Park, Pennsylvania 16802

Emmanuel P. Giannelis and Melanie Wuthenow

Material Science and Engineering Department, Cornell University, Ithaca, New York 14850

Dawn Hilton and Shawn H. Phillips

Propulsion Sciences and Advanced Concepts Division, Air Force Research Laboratory Edwards AFB, California 93524

Received February 28, 2000. Revised Manuscript Received May 8, 2000

Our continuing study of the mechanism of flammability reduction of polymer–layered-silicate nanocomposites has yielded results for polypropylene-*graft*-maleic anhydride and polystyrene–layered-silicate nanocomposites using montmorillonite and fluorohectorite. Cone calorimetry was used to measure the heat release rate and other flammability properties of the nanocomposites, under well-controlled combustion conditions. Both the polymer–layered-silicate nanocomposites and the combustion residues were studied by transmission electron microscopy and X-ray diffraction. We have found evidence for a common mechanism of flammability reduction. We also found that the type of layered silicate, nanodispersion, and processing degradation have an influence on the flammability reduction.

Introduction

Many issues are unresolved as to the mechanism(s) of the property enhancements observed for polymer–layered-silicate nanocomposites. To attempt to understand how the structural properties of these types of advanced materials influence their flammability properties, we have examined a range of nanomorphologies of polypropylene (PP)– and polystyrene (PS)–layered-silicate nanocomposites. These two commodity polymers are used in a number of commercial products which must be flame retarded. Although reduced flammability has been demonstrated for these nanocomposites, a fundamental understanding of both their unique physical properties and the reduced flammability properties is essential for nanocomposites to succeed as a flame retardant approach for virtually all polymers. This flame retardant approach via nanocomposites delivers

the unique combination of reduced flammability *with* improved mechanical properties.

Nanocomposites. Polymer–layered-silicate nanocomposites were first reported in the literature as early as 1961, when Blumstein demonstrated polymerization of vinyl monomers intercalated into montmorillonite (MMT) clay.¹ The most recent methods to prepare polymer–layered-silicate nanocomposites have primarily been developed by several other groups. In general these methods (shown in Figure 1) achieve molecular-level incorporation of the layered silicate (e.g. montmorillonite clay or synthetic layered silicate) in the polymer by addition of a modified silicate either to a polymerization reaction (in situ method),^{2–4} to a solvent-swollen polymer (solution blending),⁵ or to a polymer melt (melt blending).^{6,7} Additionally, a method has been developed

[†] Certain commercial equipment, instruments, materials, services, or companies are identified in this paper in order to specify adequately the experimental procedure. This in no way implies endorsement or recommendation by NIST.

[‡] Fire Science Division, Building and Fire Research Laboratory.

[§] Polymer Division, Materials Science and Engineering Laboratory.

^{||} The contributions of the National Institute of Standards and Technology authors are not subject to U.S. copyright.

- (1) Blumstein, A. *Bull. Chim. Soc.* **1961**, 899.
- (2) Usuki, A.; Kojima, Y.; Kawasumi, M.; Okada, A.; Fukushima, Y.; Kurauchi, T.; Kamigaito, O. *J. Mater. Res.* **1993**, 8, 1179.
- (3) Lan, T.; Pinnavaia, T. J. *Chem. Mater.* **1994**, 6, 2216.
- (4) Usuki, A.; Kato, M.; Okada, A.; Kurauchi, T. *J. App. Polym. Sci.* **1997**, 63, 137.
- (5) Jeon, H. G.; Jung, H. T.; Lee, S. D.; Hudson, S. *Polymer Bulletin* **1998**, 41, 107.
- (6) Giannelis, E. *Adv. Mater.* **1996**, 8, 29.
- (7) Fisher, H.; Gielgens, L.; Koster, T. *Nanocomposites from Polymers and Layered Minerals*; TNO-TPD Report, 1998.

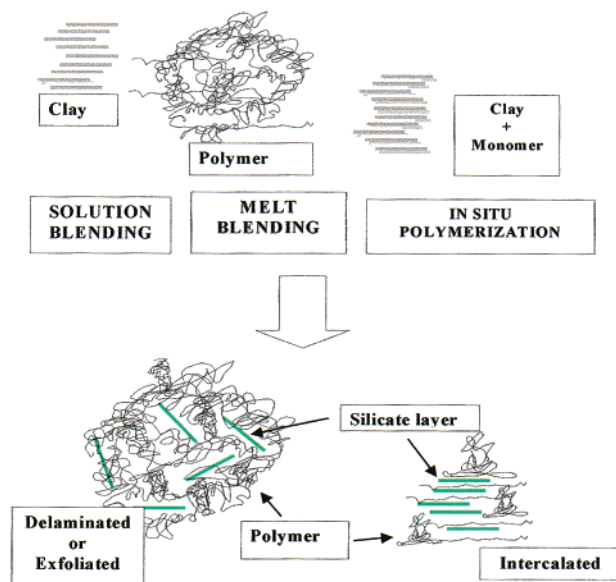


Figure 1. Schematic representation of various methods (solution blending, melt blending, and in situ polymerization) used to prepare polymer-layered-silicate nanocomposites. The delaminated (or exfoliated) and intercalated morphologies are shown.

to prepare the layered silicate by polymerizing silicate precursors in the presence of a polymer.⁸

Two terms (*intercalated* and *delaminated*) are used to describe the two general classes of nanomorphology that can be prepared. Intercalated structures are self-assembled, well-ordered multilayered structures where the extended polymer chains are inserted into the gallery space between parallel individual silicate layers separated by 2–3 nm (see Figure 2). The delaminated (or exfoliated) structures result when the individual silicate layers are no longer close enough to interact with the adjacent layers' gallery cations.⁹ In the delaminated cases the interlayer spacing can be on the order of the radius of gyration of the polymer; therefore, the silicate layers may be considered to be well-dispersed in the organic polymer. The silicate layers in a delaminated structure may not be as well-ordered as in an intercalated structure. Both of these hybrid structures can also coexist in the polymer matrix; this mixed nanomorphology is very common for composites based on smectite silicates and clay minerals.¹⁰ X-ray diffraction (XRD) measurements can be used to characterize these nanostructures if diffraction peaks are observed in the low-angle region: such peaks indicate the *d* spacing (basal spacing) of ordered–intercalated and ordered–delaminated nanocomposites. However, if the nanocomposites are disordered, no peaks are observed in the XRD, due to loss of the structural registry of the layers, the large *d* spacings (>10 nm), or both. Thus, XRD of nanocomposites has limitations because a disordered, layered silicate can either be delaminated

or intercalated. In such cases, transmission electron microscopy (TEM) combined with XRD will more accurately characterize these materials.

Polymer-layered-silicate nanocomposites have unique properties when compared to conventional filled polymers.⁶ For example, the mechanical properties of a Nylon-6-layered-silicate nanocomposite, with a silicate mass fraction of only 5%, show excellent improvement over those for pure Nylon-6. The nanocomposite exhibits increases of 40% in tensile strength, 68% in tensile modulus, 60% in flexural strength, and 126% in flexural modulus. The heat distortion temperature (HDT) is also increased, from 65 to 152 °C, and the impact strengths are lowered by just 10%.¹¹

The mechanical properties of aliphatic amine cured epoxy-layered-silicate nanocomposites, reported recently by Wang and Pinnavaia, reveal an improvement of 400% or more in tensile modulus and tensile strength and a substantial increase in the strain-at-break.¹² Decreased gas permeability and increased solvent resistance also accompany the improved physical properties.⁶ Finally, polymer-layered-silicate nanocomposites often exhibit increased thermal stability^{13,14} and, as will be discussed below, reduced flammability.^{15–20}

Thermal Stability. Blumstein first reported the improved thermal stability of a polymer-layered-silicate nanocomposite that combined poly(methyl methacrylate) (PMMA) and montmorillonite clay.²¹ Although this clay-rich nanocomposite (mass fraction ~10% intercalated PMMA) undoubtedly exhibits mechanical properties dominated by the inorganic phase, the indications of enhanced polymer thermal properties are clear. Blumstein showed that PMMA inserted (*d* spacing increase of 0.76 nm) between the lamellae of montmorillonite clay resisted thermal degradation under conditions that would otherwise completely degrade pure PMMA (refluxing decane, 215 °C, N₂, 48 h). These PMMA nanocomposites were prepared by free radical polymerization of methyl methacrylate (MMA) intercalated in the clay. Thermogravimetric analysis (TGA) reveals that both linear PMMA and cross-linked PMMA intercalated into Na⁺ montmorillonite have a 40–50 °C higher decomposition temperature. Blumstein argues that the stability of the PMMA nanocomposite is due not only to its different structure but also to restricted thermal motion of the PMMA in the gallery.

The first mention of the potential flame retardant properties of these types of materials appears in a 1976 Unitika patent application on Nylon-6 layered-silicate

(12) Wang, Z.; Pinnavaia, T. J. *Chem. Mater.* **1998**, *10*, 1820.

(13) Burnside, S. D.; Giannelis, E. P. *Chem. Mater.* **1995**, *7*, 1597.

(14) Lee, J.; Takekoshi, T.; Giannelis, E. *Mater. Res. Soc. Symp. Proc.* **1997**, *457*, 513.

(15) Gilman, J. W.; Kashiwagi, T.; Lichtenhan, J. D. *SAMPE J.* **1997**, *33*, 40.

(16) Gilman, J.; Kashiwagi, T.; Lichtenhan, J. *Proceedings of 6th European Meeting on Fire Retardancy of Polymeric Materials*; FRPM '97, September 1997, 19.

(17) Gilman, J.; Kashiwagi, T.; Lomakin, S.; Giannelis, E.; Manias, E.; Lichtenhan, J.; Jones, P. *Fire Retardancy of Polymers: the Use of Intumescence*; The Royal Society of Chemistry: Cambridge, 1998; pp 203–221.

(18) Inoue, H.; Hosokawa, T., Japan Patent Application (Showa Denko K. K., Japan) Jpn. Kokai tokkyo koho JP 10 81,510 (98 81,510), 1998.

(19) Takekoshi, T.; Fouad, F.; Mercx, F. P. M.; De Moor, J. J. M. US patent 5,773,502. Issued to General Electric Co., 1998.

(20) Okada, K. (Sekisui) Japan Patent 11-228748, 1999.

(21) Blumstein, A. *J. Polym. Sci.* **1965**, *A3*, 2665.

(8) Carrado, K. A.; Langui, X. *Microporous Mesoporous Mater.* **1999**, *27*, 87.

(9) Lan, T.; Pinnavaia, T. J. *Chem. Mater.* **1994**, *6*, 2216.

(10) For definitions and background on layered silicate and clay minerals, see: *Kirk-Othmer Encyclopedia of Chemical Technology*, 4th ed.; Kroschurtz, J. S., Ed.; John Wiley and Sons: New York, 1993; Vol. 6.

(11) Kojima, Y.; Usuki, A.; Kawasumi, M.; Okada, A.; Fukushima, Y.; Kurauchi, T.; Kamigaito, O. *J. Mater. Res.* **1993**, *8*, 1185.

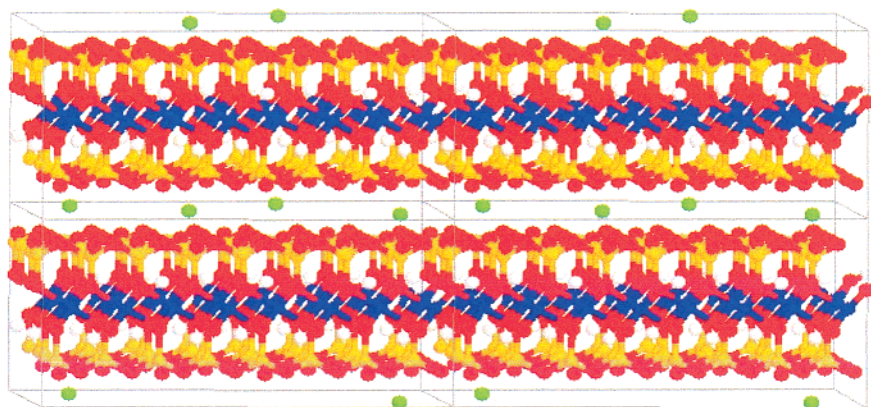


Figure 2. Molecular representation of sodium montmorillonite, showing two aluminosilicate layers with the Na^+ cations in the interlayer gap or gallery. The octahedral (O_h) alumina layer is shown as blue aluminum atoms surrounded by red oxygen atoms. The tetrahedral (T_d) silicate layers are shown as yellow silicon atoms surrounded by red oxygen atoms. Hydrogen atoms are white and sodium (Na^+) cations are shown in green.

(montmorillonite) nanocomposites.²² However, not until more recent studies did the serious evaluation of the flammability properties of these materials begin.⁶

Improvement in thermal stability similar to that reported by Blumstein for both poly(dimethylsiloxane) (PDMS) and polyimide nanocomposites has also been observed. In the case of PDMS, the nanocomposite was not prepared by in situ polymerization in sodium montmorillonite but by melt intercalation of silanol-terminated PDMS into dimethyl ditallow ammonium-treated montmorillonite.¹³ In contrast to Blumstein's materials, this nanocomposite contained *primarily* PDMS (mass fraction 90%) and only a 10% mass fraction of montmorillonite. Despite the low clay content, the disordered–delaminated nanostructure shows an increase of 140 °C in decomposition temperature compared to the pure PDMS elastomer. In view of the improved barrier properties observed for other polymer nanocomposites, this increased thermal stability was attributed to hindered diffusion of volatile decomposition products within the nanocomposite. The TGA data for several aliphatic polyimide–layered-silicate nanocomposites also shows improved thermal stability as manifested in higher decomposition temperatures. Self-extinguishing flammability behavior was reported while burning the aliphatic polyimide–layered-silicate nanocomposite¹⁴ and polycaprolactone nanocomposite.⁶ Recent work done in our laboratories, using Cone calorimetry and radiative gasification experiments, has also shown the improved flammability behavior of a number of other polymer–layered-silicate nanocomposites.^{15,17,23–24}

We report here on our continuing study of the mechanism of flammability reduction of polymer–layered-silicate nanocomposites, with recent results for polypropylene-*graft*-maleic anhydride (PPgMA) and polystyrene–layered-silicate nanocomposites using montmorillonite and fluorohectorite. Cone calorimetry was used to

measure the heat release rate (HRR) and other flammability properties of the nanocomposites, under well-controlled combustion conditions. Both the polymer–layered-silicate nanocomposites and the combustion residues were studied by TEM and XRD. We have found evidence for a common mechanism of flammability reduction. We also found that the type of layered silicate, level of dispersion, and processing degradation have an influence on the magnitude of the flammability reduction.

Experimental Section

General Procedures. Polystyrene (PS, Dow Styron 612) was dried in an air-flow oven prior to use. Polypropylene (PP, 6523, General Polymers) and polypropylene-*graft*-maleic anhydride (PPgMA, Aldrich, 0.4%²⁵ mass fraction MA) were dried for 2 h at 65 °C in an air-flow oven and then stored over silica gel and P_2O_5 before use. Organically treated layered silicates (tetradecylammonium fluorohectorite, C14-FH; octadecylammonium montmorillonite, C18-MMT; and dioctadecyldimethylammonium montmorillonite, 2C18-MMT) were prepared using a literature procedure.²⁶

Preparation of PS–Layered-Silicate Nanocomposites. PS–layered-silicate nanocomposite samples were prepared using one of the following three techniques.

A. Solvent Intercalation. A mixture of a PS–toluene solution (Dow Styron-612, M_n ²⁷ 100 000 g/mol, PS mass fraction 3–10%) and an organically treated layered silicate (mass fraction of layered silicate 3%, relative to PS) was ultrasonicated for up to 5 min until a good suspension was created. The solvent was then evaporated for several hours at ambient temperature in a fume hood, yielding a very viscous gel. The gel was placed in a vacuum oven at 70 °C for 2–5 h to evaporate the remaining solvent.²⁸

B. Static Melt Intercalation. PS (dried, powdered) and organically treated layered-silicate (dried) were mixed and

(25) All formulation percentages (%) are in mass fraction %.

(26) Vaia, R. A.; Teukolsky, R. K.; Giannelis, E. P. *Chem. Mater.* **1994**, *6*, 1017.

(27) According to ISO 31-8, the term “Molecular Weight” has been replaced by “Relative Molecular Mass”, symbol M_r . Thus, if this nomenclature and notation were used here, $M_{r,n}$ instead of the historically conventional M_n for the average molecular weight (with similar notation for M_w , M_z , M_v) would be used. It would be called the “Number-Average Relative Molecular Mass”. The conventional notation, rather than the ISO notation, has been employed here.

(28) Note: Most of the toluene must be removed *prior* to putting the sample into the vacuum oven. If large amounts of toluene remain, the vigorous boiling away of the solvent will result in an inhomogeneous sample.

(29) Babrauskas, V. *Fire Mater.* **1995**, *19*, 243.

(22) Fujiwara, S.; Sakamoto, T. Kokai Patent Application, no. SHO 511976-109998, 1976.

(23) (a) Gilman, J. W.; Kashiwagi, T.; Brown, J. E. T.; Lomakin, S.; Giannelis, E. P.; Manias, E. *Proceedings of 43rd International SAMPE Symposium and Exhibition*, May 1998, 1053. (b) Gilman, J. W.; Kashiwagi, T.; Nyden, M.; Brown, J. E. T.; Jackson, C. L.; Lomakin, S.; Giannelis, E. P.; Manias, E. *Chemistry and Technology of Polymer Additives*; Blackwell Scientific, Oxford, 1999; pp 249–265.

(24) Gilman, J. W. *Appl. Clay Sci.* **1999**, *15*, 31.

ground together in a mortar and pestle. The mixed powder was heated at 170 °C for 2–6 h in a vacuum. The material was stirred once halfway through the annealing/melt intercalation process.

C. Extrusion Melt Intercalation. PS (dried, powdered) and organically treated layered silicate (dried) were premixed and blended/extruded using a DSM miniextruder under N₂ at 150–170 °C for 2–4 min.

Preparation of PPgMA–Layered-Silicate Nanocomposites. PPgMA and an organically treated layered silicate (dimethylbis(hydrogenated tallow)ammonium MMT) were blended in a mixing head (Haake Rheomix 600 (69 cm³ capacity), Haake Rheocord 9000 system). The polymer and layered silicate were blended at 200 °C for 10 min. Upon completion of blending, the molten polymer was removed and allowed to cool. The PPgMA–layered-silicate nanocomposite (14–15 g) was then compression molded, at 180 °C and 3 metric tons of pressure, to give a 7.35 cm diameter × 0.37 cm thick disk. These disks were then used for Cone calorimetry testing.

X-ray Diffraction Measurements. XRD data were collected on a Philips diffractometer using Cu K α radiation, (λ = 0.1505945 nm). Powdered char samples were ground to a particle size of less than 40 μ m.

Transmission Electron Microscopy. Bright field TEM images of PPgMA–layered-silicate nanocomposites and the corresponding combustion chars, were obtained at 120 kV, under low-dose conditions, with a Philips 400T. The PPgMA–layered-silicate nanocomposite samples were cryomicrotomed with a diamond knife at –110 °C to give sections with a nominal thickness of 70 nm. Combustion chars were broken into small pieces, embedded in an epoxy resin (Epofix), and cured overnight at room temperature. Ultrathin sections were prepared with a 45° diamond knife at room temperature using a DuPont-Sorvall 6000 ultramicrotome. The sections were transferred dry to carbon-coated Cu grids of 200 mesh. The contrast between the layered silicates and the polymer phase was sufficient for imaging, so heavy metal staining of sections prior to imaging was not required. Direct observation of the PS nanocomposite structure was realized by bright field TEM of nanocomposite films (0.5–1.5 μ m thick) under strain in a JEOL-1200EX operating at 120 kV. The PS–fluorohectorite-based materials were microtomed from bars using a diamond knife to give 50 nm thick sections which were placed onto copper grids. MMT-based materials were spin cast directly onto copper grids. The contrast between the silicon-containing phase and the polymer was sufficient for imaging, and no staining was required.

Flammability Measurements. Evaluations of flammability were achieved using the Cone calorimeter. The tests were performed at an incident heat flux of 35 kW/m² using the Cone heater.²⁹ Peak heat release rate, mass loss rate, and specific extinction area (SEA) data, measured at 35 kW/m², are reproducible to within $\pm 10\%$. The carbon monoxide and heat of combustion data are reproducible to within $\pm 15\%$. The uncertainties for the Cone calorimeter are based on the uncertainties observed while thousands of samples combusted to date were evaluated. The Cone data reported here are the average of two or three replicated experiments. The errors (1 σ) are shown as error bars on the plots of the Cone data.

Results

The Cone calorimeter is one of the most effective bench-scale methods for studying the flammability properties of materials. Fire-relevant properties, measured by the Cone calorimeter, such as heat release rate (HRR), *peak* HRR, and smoke and carbon monoxide yield, are vital to the evaluation of the fire safety of materials.³⁰ We have characterized the flammability properties of a variety of polymer–layered-silicate

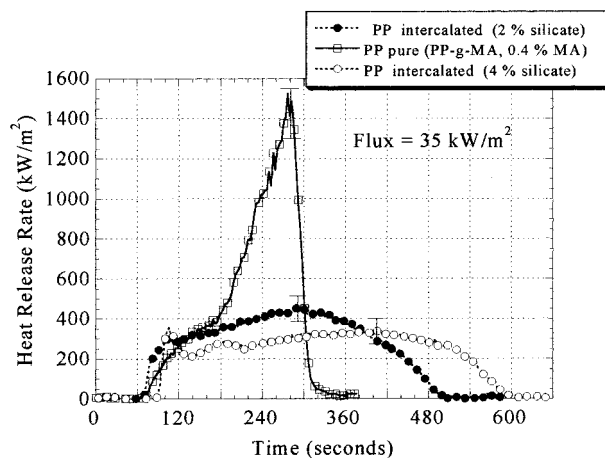


Figure 3. Comparison of the heat release rate (HRR) plots for pure PPgMA and two PPgMA–layered-silicate nanocomposites, at 35 kW/m² heat flux, showing a 70–80% reduction in peak HRR for the nanocomposites with a mass fraction of only 2% or 4% layered silicate, respectively.

nanocomposites, under firelike conditions,²⁹ using the Cone calorimeter. We first observed reduced flammability for Nylon-6–layered-silicate nanocomposites.¹⁵ Subsequent preliminary investigations of polystyrene PS– and PPgMA–layered-silicate nanocomposites showed similar reductions in flammability,¹⁶ as did thermoset polymer nanocomposites made from vinyl esters and epoxies.²³

PP–Layered-Silicate Nanocomposites. In this work, we describe our most recent study of the flammability and structure properties of nanocomposites prepared from PPgMA, PS, and Nylon-6. We have prepared PPgMA–layered-silicate nanocomposites using PPgMA (mass fraction of MA 0.4%), known to be miscible with pure PP, and dimethylbis(hydrogenated tallow)ammonium MMT. Researchers at Toyota have also reported on PP–layered-silicate nanocomposites and have demonstrated their improved physical properties. These materials were also prepared using PPgMA to disperse the silicate.³¹

The HRR plots for PPgMA and PPgMA–MMT nanocomposites (silicate mass fraction 2% and 4%) at 35 kW/m² heat flux are shown in Figure 3 and are typical of those found for all the nanocomposites in Table 1. The PPgMA–MMT-silicate (4%) nanocomposite has a 75% lower HRR than the pure PPgMA. Comparison of the Cone calorimeter data in Table 1, for the Nylon-6, PS, and PPgMA nanocomposites, reveals that the specific heat of combustion (H_c), specific extinction area (SEA, a measure of smoke yield), and carbon monoxide yields are unchanged; this suggests that the source of the improved flammability properties of these materials is due to differences in condensed-phase decomposition processes and not to a gas-phase effect. For comparison, the flammability properties of PS flame retarded with decabromodiphenyloxide (DBDPO) and Sb₂O₃ are also shown in Table 1. These data show that the effect of bromine is primarily in the gas-phase, as evidenced by the lower heat of combustion and higher CO yield typical of incomplete combustion. The primary parameter responsible for the lower HRR of the nanocompos-

(30) (a) Babrauskas, V.; Peacock, R. D. *Fire Safety J.* **1992**, *18*, 255.

(31) Kawasumi, M.; Hasegawa, N.; Kato, M.; Usuki, A.; Okada, A. *Macromolecules* **1997**, *30*, 6333.

Table 1. Cone Calorimeter Data

sample (structure)	% residue yield (± 0.5)	peak HRR, (kW/m ²) ($\Delta\%$)	mean HRR, (kW/m ²) ($\Delta\%$)	mean H_c , MJ/kg	mean SEA, m ² /kg	mean CO yield, kg/kg
Nylon-6	1	1010	603	27	197	0.01
Nylon-6-silicate nanocomposite 2% (delaminated)	3	686 (32)	390 (35)	27	271	0.01
Nylon-6-silicate nanocomposite 5% (delaminated)	6	378 (63)	304 (50)	27	296	0.02
PS	0	1120	703	29	1460	0.09
PS-silicate mix 3% (immiscible)	3	1080	715	29	1840	0.09
PS-silicate nanocomposite 3% (intercalated-delaminated)	4	567 (48)	444 (38)	27	1730	0.08
PS w/ DBDPO/Sb ₂ O ₃ 30%	3	491 (56)	318 (54)	11	2580	0.14
PPgMA	5	1525	536	39	704	0.02
PPgMA-silicate nanocomposite 2% (intercalated-delaminated)	6	450 (70)	322 (40)	44	1028	0.02
PPgMA-silicate nanocomposite 4% (intercalated-delaminated)	12	381 (75)	275 (49)	44	968	0.02

^a Heat flux, 35 kW/m². H_c , specific heat of combustion; SEA, specific extinction area. Peak heat release rate, mass loss rate, and SEA data, measured at 35 kW/m², are reproducible to within $\pm 10\%$. The carbon monoxide and heat of combustion data are reproducible to within $\pm 15\%$.

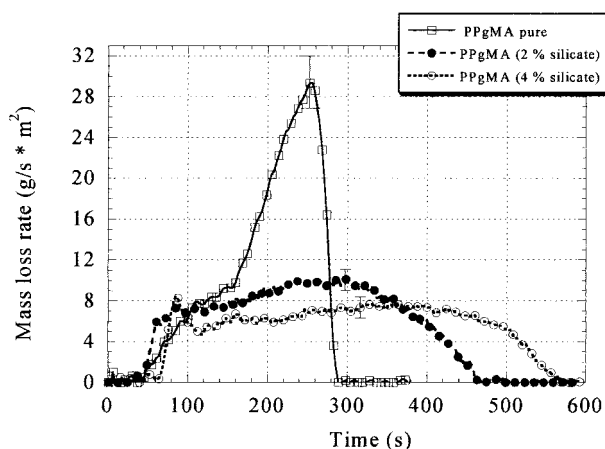


Figure 4. Mass loss rate plots for PPgMA and two PPgMA-layered-silicate nanocomposites.

ites is the mass loss rate (MLR) during combustion, which is significantly reduced from those values observed for the pure polymers (Figure 4).

Previously we reported a 54% lower peak HRR for a PPgMA-MMT nanocomposite made by compression molding.¹⁶ The samples presented here were prepared using a mixing head, which dispersed the layered-silicate particles into the molten polymer under shear. The TEM of the resulting PPgMA-MMT (4%) nanocomposite in Figure 5 shows that the PPgMA nanocomposite has a mixed nanomorphology. Individual silicate layers, along with two and three layer stacks, are observed to be well-dispersed (exfoliated) in the polymer matrix. In addition, some larger intercalated tactoids (multilayer particles) are also visible in an enlarged region by TEM (Figure 6); this sample also showed a peak by XRD corresponding to a d spacing of 3.5 nm. This delaminated-intercalated PPgMA nanocomposite gave a 75% lower peak HRR.

Each of the thermoplastic nanocomposite systems we have examined shows essentially the same behavior when evaluated in the Cone calorimeter. Furthermore, comparison of the residue yields (taken after combustion in the Cone calorimeter) for the each of the nanocomposites in Table 1 reveals a small improvement in the carbonaceous char yields, once the presence of the silicate in the residue is taken into account. These data

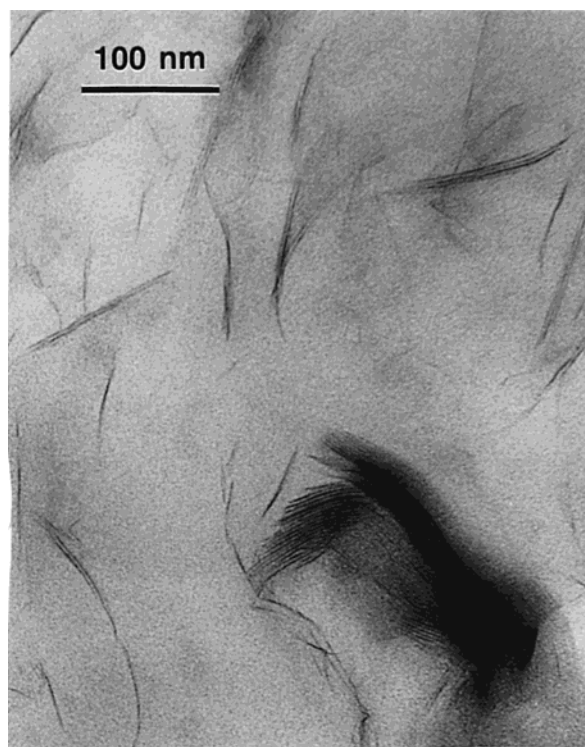


Figure 5. TEM of PPgMA-layered-silicate (mass fraction 4%) nanocomposite: with exfoliated single, double, and triple layers as well as a multilayer tactoid.

indicate that the mechanism of flame retardancy may be very similar for each of the systems studied. However, the lower flammability is not due to retention of a large fraction of fuel, in the form of carbonaceous char, in the condensed phase. Support for a common fire retardant mechanism comes from TEM and XRD analysis of chars from a variety of nanocomposites. TEM images of sections of the combustion chars from the PPgMA-MMT nanocomposite (4%) are shown in Figure 7. In the Nylon-6-layered-silicate char a multilayered carbonaceous-silicate structure is seen after combustion, with the silicate sheets forming a large array of fairly even layers.¹⁶ In the Nylon-6-layered-silicate nanocomposite the delaminated nanostructure appears to collapse during combustion and yields a peak in the XRD at 1.38 nm (Figure 8).¹⁶ The new nanocomposite

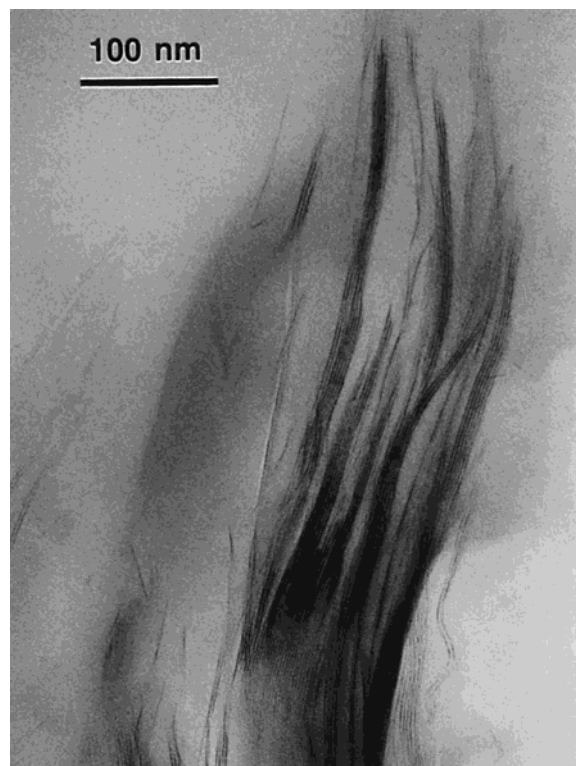


Figure 6. TEM of an intercalated tactoid (d spacing 3.5 nm) of PPgMA-layered-silicate (mass fraction 4%) nanocomposite.

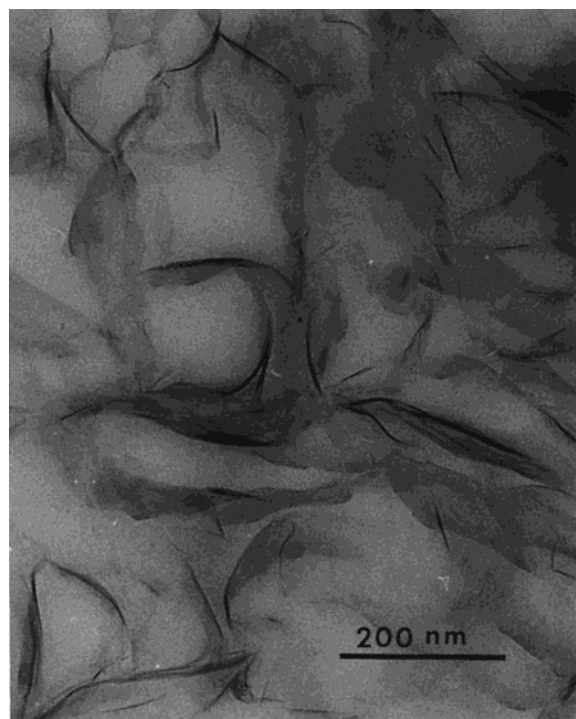


Figure 7. TEM of the combustion char from the PPgMA-MMT nanocomposite (4%) showing the carbonaceous-silicate multilayered structure.

structure present in the resulting combustion residue appears to enhance the performance of the residue through reinforcement of the carbonaceous char layer. This is analogous to the enhancement of properties of the pure polymer. This multilayered carbonaceous-silicate structure may act as an excellent insulator and mass transport barrier, slowing the escape of the volatile

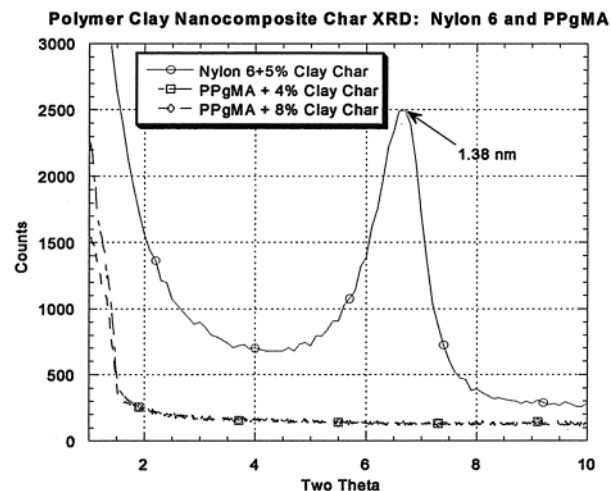


Figure 8. XRD of the combustion chars from the Nylon-6 MMT nanocomposite and the PPgMA-MMT nanocomposite.

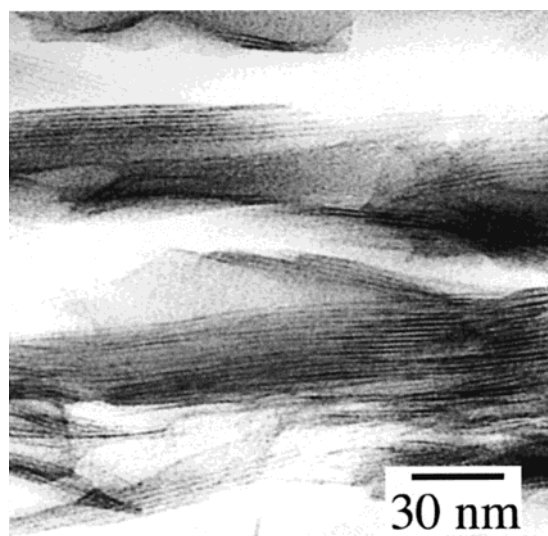


Figure 9. TEM of PS (3% C14-FH) showing an intercalated nanomorphology with a layer spacing of 3.2 nm.

products generated during decomposition.¹⁶ Analysis of combustion residues from two epoxy nanocomposites, by XRD, shows that the interlayer spacing of both chars is 1.3 nm.¹⁶ A few layered carbonaceous-silicate structures are also observed in the PPgMA-MMT char, but as Figure 7 shows, individual silicate layers are also dispersed throughout the carbonaceous char and no peak in XRD is observed (Figure 8).

Effect of Structure on Flammability of PS-Layered-Silicate Nanocomposites. To understand how the structure of PS nanocomposites influences flammability properties, we examined a range of nanomorphologies of PS-layered silicates. We looked at PS with a primary ammonium-treated fluorohectorite (PS C14-FH, silicate mass fraction 3%) and PS with a quaternary ammonium-treated MMT (PS 2C18-MMT, silicate mass fraction 3%). These two layered silicates disperse differently in PS. The TEM image (Figure 9) of the PS C14-FH, prepared by static melt intercalation, shows that it is a neatly intercalated nanocomposite. The TEM image for the PS 2C18-MMT sample, prepared by static melt intercalation (Figure 10), shows that it contains *both* intercalated MMT and delaminated

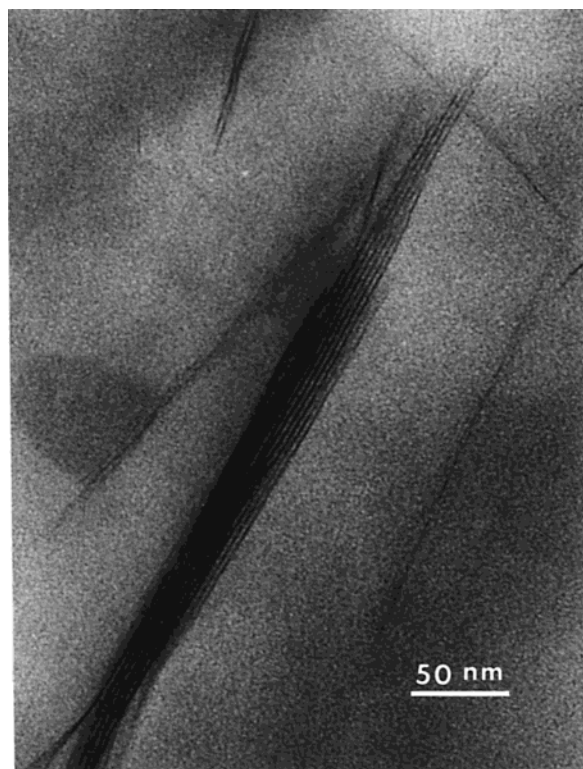


Figure 10. TEM of PS (3% 2C18-MMT). About 25% of the MMT layers are delaminated with the remaining MMT intercalated with a layer spacing of 3.1 nm.

MMT layers, similar to the PPgMA nanocomposite. TEM studies³² of the PS 2C18-MMT nanocomposites show that typically 25% of the MMT layers are homogeneously dispersed in the PS matrix (in single or 2–3 layer stacks), while the remaining organo-layered silicate forms ordered–intercalated tactoids that consist of many parallel silicate layers. We note that the MMT plates with shorter aspect ratios were better dispersed, i.e., in single or 2–3 layer stacks, and the larger aspect ratio plates were found in the intercalated tactoids. These PS nanocomposites also differ in that FH is a synthetic layered magnesium silicate with fluorine substituted for hydroxyl groups (unit cell formula $Z^{+}_{1.6}[\text{Li}_{1.6}\text{Mg}_{4.4}(\text{Si}_{8.0}\text{O}_{20}\text{F}_4)]$, where Z^{+} is the exchange cation) with a high aspect ratio (500:1 to 4000:1, FH plate diameter 4–5 μm), while MMT, is a layered aluminosilicate (unit cell formula $Z^{+}_{0.86}[\text{Mg}_{0.86}\text{Al}_{3.14}(\text{Si}_{8.0}\text{O}_{20}\text{OH}_4)]$) with a lower aspect ratio (100:1 to 1000:1, MMT plate diameter 0.1–1 μm).

Figure 11 shows the heat release rate data for the PS nanocomposites (MMT and FH) and two control samples, pure PS and PS mixed with sodium montmorillonite, which gives an immiscible, conventional, filled composite. Surprisingly, the PS 2C18-MMT and PS C14-FH behave very differently. The PS C14-FH has, within experimental uncertainty, no effect on the peak HRR, whereas the PS 2C18-MMT has a 60% lower peak HRR as compared to the pure PS or the PS mixed with NaMMT (immiscible). Since the two nanocomposites have different chemical formulas of the layered silicate, different aspect ratios, and different nanomorphologies,

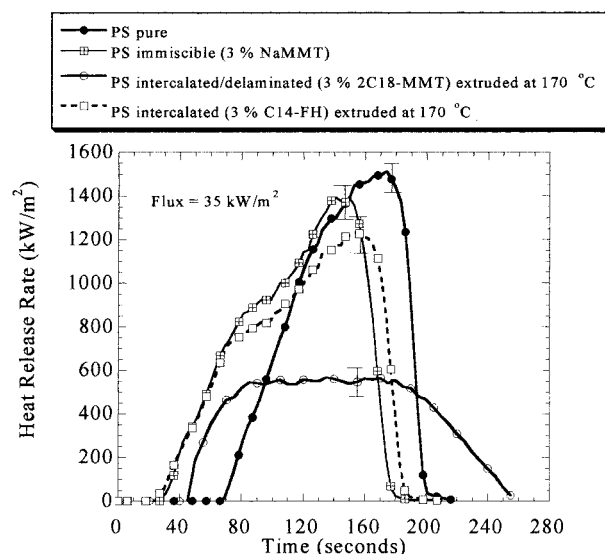


Figure 11. Heat release rate (HRR) plots for pure PS; PS with NaMMT, an immiscible composite; PS with bis-C18 quaternary ammonium-treated MMT; and PS with C14 primary ammonium-treated FH, at 35 kW/m² heat flux.

it is difficult to determine the exact reason for their very different flammability. However, in a previously reported aliphatic polyimide nanocomposite system, both FH and MMT nanocomposites were found to have the same increase in thermal stability (by TGA).¹⁴ The possibility exists that only the delaminated PS nanocomposites have reduced flammability; however, in a previous study we found that both epoxy and vinyl ester intercalated nanocomposites (with MMT) show reduced flammability. The lack of effectiveness for this intercalated PS-FH nanocomposite is in agreement with results reported by Showa-Denko on PBT, Nylon-6, and Nylon-6,6 nanocomposites using a similar layered silicate, fluorinated synthetic mica (FSM).¹⁸ Fluorinated synthetic mica has a high aspect ratio and chemical composition like FH. The flammability of Nylon-6-FSM nanocomposites was tested using the UL 94 test, and the results showed that more than 50% of the FSM had to be uniformly dispersed (delaminated) in stacks of five or fewer layers for a V-2 or V-0 (self-extinguishing) rating to be obtained.¹⁸ Our view of the nanocomposite's flame retardant mechanism is that a high-performance carbonaceous–silicate char builds up on the surface during burning; this insulates the underlying material and slows the mass loss rate of decomposition products. This residue layer forms as the polymer burns away and the silicate layers reassemble into the multilayer char observed in the TEM. We have shown reduced flammability for both delaminated and intercalated MMT nanocomposites. However, it appears that the intercalated-FH nanocomposites are not effective. Possibly, the large aspect ratio of the FH interferes with this reassembly process. However, the potential difference in chemical reactivity of MMT versus FH cannot be ruled out as a significant factor either.

Figure 12 shows the effect of processing conditions on the flammability of PS nanocomposites. When the PS 2C18-MMT nanocomposite is prepared via melt blending in an extruder (at 170 °C, under N₂ or vacuum) or by solvent (toluene) blending, an intercalated–delaminated nanostructure results, which has reduced

(32) Exhaustive visual inspection of 100 TEM images from PS-2C18-MMT was carried out to determine the number of the single, double, triple, or multiple layer particles present in the nanocomposite.

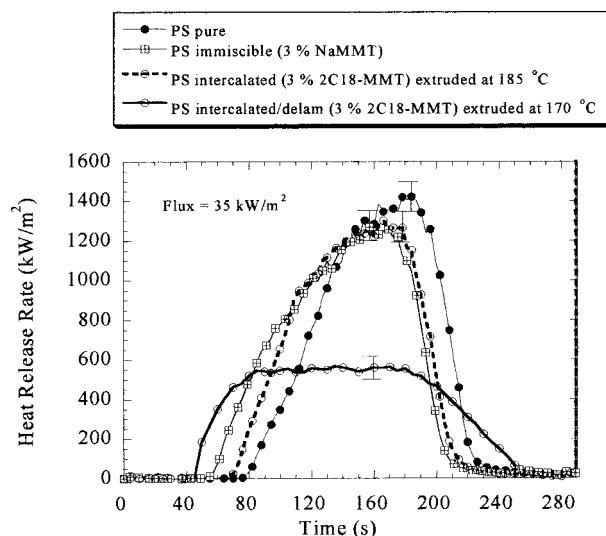


Figure 12. Heat release rate (HRR) plots for pure PS, PS with NaMMT, an immiscible composite; PS with bis-C18 quaternary ammonium-treated MMT; and PS with bis-C18 quaternary ammonium-treated MMT processed at 185 °C.

flammability. However, if the extrusion conditions include high temperatures and if air is not excluded, the nanocomposite that forms has no improvement in flammability, as the data in Figure 12, for PS 2C18-MMT extruded at 185 °C, shows. This may be due to degradation of the polymer during the extrusion, caused by thermal degradation of the organic treatment present on the clay.^{33,34} This degradation works in opposition to the flame retardancy mechanism of the clay, in that it lessens the protective effect that the clay layers provide the polymer nanocomposite. Indeed, the polydispersity (PDI, M_w/M_n from GPC) of this sample is 2.40; this is a significant increase from the PDI of 1.8 for the immiscible PS–NaMMT sample, which was extruded under identical conditions. The fact that the organic-treated MMT has a much larger change in PDI than the NaMMT sample, after extrusion at 185 °C in air, indicates that the organic treatment may play a role in the degradation reactions that broaden the PDI. The Hofmann degradation of tetraalkylammonium ions,³⁵ which forms the less substituted olefin and the amine, could supply olefin at these temperatures that could combine with oxygen to give peroxoradicals. These radicals and other mechano-radicals would broaden the

PDI through typical free radical processes. Additional studies of this type of degradation are underway in our laboratory.

Summary

All MMT-based nanocomposite systems reported so far show reduced flammability. Peak HRR is reduced by 50%–75% for Nylon-6, PS, and PPgMA nanocomposites. We have shown that the MMT must be nano-dispersed for it to affect the flammability. However, the clay need not be completely delaminated for it to affect the flammability of the nanocomposite. We have observed that an intercalated PS–fluorohectorite nanocomposite is *ineffective* at reducing the flammability of PS, possibly due to the large aspect ratio of fluorohectorite. However, the potential difference in chemical reactivity of fluorohectorite cannot be ruled out as a significant factor. We have evidence of an antagonistic interaction between high processing temperatures and the alkylammonium MMT, which causes an increase in the PDI in PS–MMT nanocomposites during processing. Our view of the general nanocomposite flame retardant mechanism is that a *high-performance* carbonaceous–silicate char builds up on the surface during burning; this insulates the underlying material and slows the mass loss rate of decomposition products.

Many issues are unresolved as to the mechanism of the property enhancements (flammability and physical) observed in polymer–layered-silicate nanocomposites. When they are resolved, nanocomposites may fulfill the requirements for a high-performance additive-type flame retardant system, i.e., one that reduces flammability while improving the other performance properties of the final formulated product. This may be accomplished either as a single flame retardant additive or in combination with other flame retardant additives. Indeed, several patents and publications have taken this latter approach to successfully improve both the flammability and the mechanical properties of many polymer systems.^{18–20}

Acknowledgment. The authors would like to thank Dr. Richard Lyon and the Federal Aviation Administration for partial funding of this work, through Inter-agency Agreement DTFA0003-92-Z-0018. We would also like to thank Ms. Lori Brassell for sample preparation and data analysis, Mr. Michael Smith for Cone calorimeter analysis, Dr. James Cline for use of XRD facilities, and Dr. Marc Nyden for the montmorillonite structure. We would also like to express our gratitude to Southern Clay Products Inc. for the organic-modified layered silicates.

CM0001760

(33) Krishnamorti, R. Personal communication.

(34) Gilman, J. W.; Morgan, A. B.; Harris, R. H.; Trulove, P. C.; DeLong, H. C.; Suttu, T. E. *PMSE Preprints*, in press.

(35) Saunders, W. S., Jr. *Ionic Aliphatic Reactions*; Prentice Hall: Englewood Cliffs, 1965; 67–73.